Applied Surface Science 317 (2014) 167–171

Contents lists available at ScienceDirect

Applied Surface Science

journal homepage: www.elsevier.com/locate/apsusc

Investigation of the particle size distribution of the ejected material generated during the single femtosecond laser pulse ablation of aluminium

Han Wu, Nan Zhang, Xiaonong Zhu*

Institute of Modern Optics, Nankai University, Key Laboratory of Optical Information Science and Technology, Ministry of Education, Tianjin 300071, China

ARTICLE INFO

Article history:
Received 29 March 2014
Received in revised form 19 July 2014
Accepted 3 August 2014
Available online 9 August 2014

Keywords:
Femtosecond laser deposition
Nanoparticle generation
Particle size distribution

ABSTRACT

Single femtosecond laser pulses are employed to ablate an aluminium target in vacuum, and the particle size distribution of the ablated material deposited on a mica substrate is examined with atomic force microscopy (AFM). The recorded AFM images show that these particles have a mean radius of several tens of nanometres. It is also determined that the mean radius of these deposited nanoparticles increases when the laser fluence at the aluminium target increases from 0.44 J/cm^2 to 0.63 J/cm^2. The mechanism of the laser-induced nanoparticle generation is thought to be photomechanical tensile stress relaxation. Raman spectroscopy measurements confirm that the nanoparticles thus produced have the same structure as the bulk aluminium.

1. Introduction

The generation of nanoparticles of controllable size is of considerable interest in scientific research. Nanoparticles of different elements and compounds have remarkable properties [1,2] and many important technological applications. For examples, gratings of a metallic nanoparticle microstructure can be used to enhance the efficiency of light-emitting diodes [3], and aluminium nanoparticles have been found to be good candidates for plasmonic materials in the UV region, which opens up new possibilities for extending the applications of plasmonics [4]. Although several traditional techniques to produce nanoparticles are available, over the past decade, laser ablation has been found to be an attractive and efficient method for producing nanoparticles. The generation of nanoparticles through laser ablation has a number of advantages, such as the production of a narrower size distribution [5], multicomponent nanoparticle production [6], and the direct formation of nanopillars [7]. Because a laser ablation process may be readily affected by the optical energy fluence, pulse width, and pulse repetition rate, among other parameters, one can effectively control the end products by proper selection of the experimental conditions.

The use of femtosecond laser pulses to ablate a solid target in vacuum to synthesise nanoparticles is advantageous in the following three respects. First, femtosecond laser pulses rapidly deliver sufficient energy to the target material to reach a solid-density plasma state with temperature and pressure well above the critical point, greatly reducing the thermal effect on the surface. As a result, femtosecond laser ablation can be used for nanoparticle generation from a broad range of materials. Second, unlike in nanosecond (or longer) laser pulse ablation, because of the short pulse duration, there is no interaction between the ejected plume and the femtosecond laser pulses. Third, the plume formed after the presence of the laser field expands explosively, undergoing a relatively simple physical process in vacuum.

Previous investigations in this regard mainly discuss the properties of the products obtained from laser ablation [8] and the dynamics of the flying plume [9]. (To generate adequate amount of nanoparticles, many of these studies also use multi-pulses in their laser ablation experiments, which inevitably induce a complicated physical process.) Relatively few studies have discussed the ablation mechanism based on analyses of the ablation products, such as nanoparticles of different sizes. In this case, it is better to use a single pulse to properly discuss the ablation mechanism. In multiple-pulse ablation, a crater is normally formed after the first laser pulse (and may be further altered by every following pulse); thus, the successive pulses will encounter very different target conditions in terms of surface morphology and reflectivity. This will inevitably have a significant impact on the process of the femtosecond-laser-induced nanoparticle generation. In single-pulse ablation, nanoparticle generation is more likely to undergo

* Corresponding author.
E-mail address: xnzhu1@nankai.edu.cn (X. Zhu).

http://dx.doi.org/10.1016/j.apsusc.2014.08.005
0169-4332/

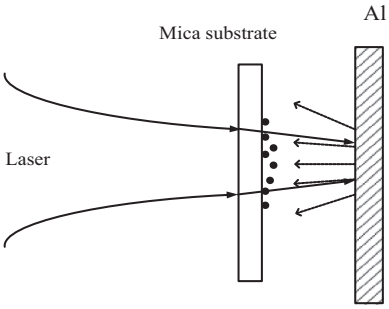

Fig. 1. Schematic of the experimental setup. The mica substrate, which is transparent to the incident laser, is used for particle collection; Al: aluminium target.

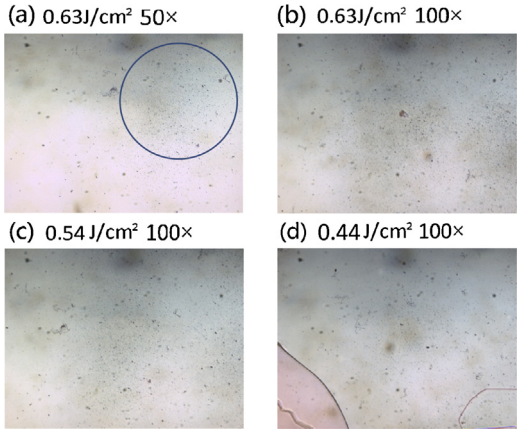

Fig. 2. Optical microscopy observations of the mica substrate covered by the deposited material generated by the single 50-fs laser pulse ablation of an aluminium target at different fluences. The fluence of the laser pulse used to ablate the target and the magnification rate for each image are presented on the left top corner of each image. Frame size: (a) 119 μm × 89.3 μm; (b)–(d) 59.5 μm × 44.65 μm.

an identical thermal process, and the number density of the particles is also greatly reduced. Therefore, the ambiguities caused by the overlap of the particles can be minimised.

In our study, a single 50-fs laser pulse ablation of an aluminium target in vacuum is implemented, and the main characteristics of the generated nanoparticles are examined using AFM and Raman spectroscopy. Consistent with a previous study [10], a single laser pulse of ~0.45 mJ in pulse energy with a central wavelength of approximately 800 nm is sufficient to produce nanoparticles with a 100-mm-focal-length lens. The size distribution of the nanoparticles peaks at 10–20 nm with variable standard deviation. Nanoparticles with large radii of several hundred nanometres are observed, which may originate from the large stress gradients [11] induced by the heating effect under a laser fluence of approximately 0.5 J/cm^2, which is a consequence of photomechanical stress relaxation [12].

2. Experimental setup

A schematic diagram of our experimental setup is shown in Fig. 1. The ablation is carried out with a Ti:sapphire femtosecond laser system (HP Spitfire, Spectra Physics Inc.), which produces ~1-mJ, 50-fs pulses at 800 nm. Using a positive lens of 100-mm focal length, we focus the input laser beam to the target at normal incidence. The spot size at the sample surface is approximately 150 μm. The particles ablated off the target are collected on the mica substrate placed parallel to the aluminium sample and perpendicular to the incident laser. To avoid optical damage, the position of the mica substrate is selected such that it experiences lower laser fluence. The distance between the mica substrate and the aluminium target is approximately 1.3 mm, which will not induce confinement of the ejected plume during the initial ablation. We measure the transmittance of the mica substrate and account for it in the fluence control. The fluence is 0.63 J/cm^2 at the target surface and can be attenuated by adjusting a half-wave plate inside the pulse compressor of the femtosecond laser system.

The target is mounted on a translation stage and is moved to a new position after each single pulse is fired to prevent the ablation sites created by different laser shots from overlapping. To avoid the possible influence of the air environment on the ablation, the experiments are conducted in vacuum (10^{-4} Pa). The mica substrate after particle deposition is first visually examined using an optical microscope (Olympus BX51) with CCD (Imaging Source DFK 41BU02) detection. The nanoparticles deposited on the mica substrate are then analysed by AFM (Veeco Nanoscope IV) in tapping mode and Raman spectroscopy (RFS 100/S Bruker) of the deposited material. The tip radius used in our AFM measurements is 10 nm.

3. Results and discussion

Fig. 2(a) shows the 50× optical microscopic image of the mica surface covered by deposited material generated during the single 50-fs laser pulse ablation of aluminium at a laser fluence of 0.63 J/cm^2. The deposited material is mainly found inside the solid circle in Fig. 2(a), with much fewer particles found outside the circle. In Fig. 2(b)–(d), the laser fluence decreases from 0.63 J/cm^2 to 0.44 J/cm^2, and the corresponding microscopic images show a decrease in the amount of the material deposited with decreasing fluence. Some of the deposited particles, observed as black dots in the optical microscopy images, have larger radii of 100 nm, which is different from the results reported in the previous studies [6]. It is noted that the site of maximum deposition is actually in line with the geometrical centre of the laser spot and the ablation crater of the aluminium target. Fig. 3 shows the AFM images of the aluminium nanoparticles deposited on the mica substrate. Fig. 3(a) presents the AFM image of the pristine mica substrate, which is used as a reference for comparison with the deposited substrates. The pristine mica has a smooth surface with a height variation of ±0.5 nm. Fig. 3(b)–(d) presents the respective AFM images of the central areas of the deposited regions shown in Fig. 2(b)–(d). Although they differ in size, all of the nanoparticles are scattered over the substrate, with relatively few lumps.

The size distributions of the aluminium nanoparticles corresponding to the three AFM images in Fig. 3(b)–(d) are shown in Fig. 4(a)–(c), respectively. For the three different laser fluences, the statistical results concerning the particle size distribution show that the radii of the deposited particles are mainly in the range of 0–100 nm, with a peak value of 10–20 nm. As the laser fluence decreases, the particle size distribution becomes narrower and more concentrated in the 10–20-nm region. The statistical data for the nanoparticle sizes for the different laser fluences are summarised in Table 1. The total number of the nanoparticles per AFM image and the particle number density are calculated. The nanoparticle size varies widely from tens of nanometres to approximately 400 nm, similar to those reported in Ref. [5]. It can be concluded that as the laser fluence decreases, both the mean and the maximum radii of the nanoparticles decrease.

It is assumed that the particles have a more cubic shape on average, and the size information obtained from AFM is relatively accurate in height but rough in width. (The longitudinal resolution of the AFM we used is ~0.1 nm, and the lateral resolution is ~10 nm, assuming it is comparable to the tip radius.) We thus take the